Kondo insulators modeled by the one-dimensional Anderson lattice: A numerical-renormalization-group study

M. Guerrero and Clare C. Yu
Department of Physics and Astronomy, University of California, Irvine, Irvine, California 92717
(Received 17 August 1994; revised manuscript received 19 December 1994)

In order to better understand Kondo insulators, we have studied both the symmetric and asymmetric Anderson lattices at half filling in one dimension using the density-matrix formulation of the numerical renormalization group. The asymmetric case is treated in the mixed-valence regime. We have calculated the charge gap, the spin gap, and the quasiparticle gap as a function of the repulsive interaction U using open boundary conditions for lattices as large as 24 sites. We find that the charge gap is larger than the spin gap for all U for both the symmetric and asymmetric cases. Ruderman-Kittel-Kasuya-Yosida interactions are evident in the f-spin–f-spin correlation functions at large U in the symmetric case, but are suppressed in the asymmetric case as the f level approaches the Fermi energy. This suppression can also be seen in the staggered susceptibility $\chi(q=2k_F)$ and it is consistent with neutron scattering measurements of $\chi(q)$ in CeNiSn.

I. INTRODUCTION

Kondo insulators are a class of rare-earth compounds that become semiconducting at low temperatures. However, they are not just ordinary semiconductors because their gaps are due to many-body interactions between extended conduction and localized electrons in the f shell. At high temperatures ($T > 100$ K), these materials behave as metals with local magnetic moments, but at low temperatures they exhibit a small gap in their excitation spectrum and behave as narrow-gap semiconductors (typically $\Delta \sim 100$ K). This class of materials includes $Ce_3Bi_4Pt_3$, CeNiSn, and SmB_6.[1] It has also been argued that the transition-metal compound FeSi is also a Kondo insulator.[1]

Theoretically, the Kondo insulators have been modeled by both the Kondo lattice and the periodic Anderson model at half filling.[2–7] In the Anderson lattice each site has a localized orbital that hybridizes with an extended band of conduction electrons. Double occupation of the localized orbital is penalized by a strong Coulomb repulsion U. The half-filled system, in which there are two electrons per site, is an insulator at zero temperature.

In the Anderson model, two distinct regimes can be considered. In the *Kondo regime,* the energy of the localized band lies well below the Fermi surface. In this case, the occupation of the localized level is very close to one and charge fluctuations in and out of the localized orbital are negligible. On the other hand, in the *mixed-valence regime,* the energy of the localized orbital lies very close to the Fermi level and electrons can hop into and out of the localized orbital. As a result, charge fluctuations are important and the average occupancy of the localized orbital is less than one.

Most of the theory on Kondo insulators has treated them in the Kondo regime or assumed particle-hole symmetry or both.[2–7] (The symmetric Anderson lattice has particle-hole symmetry while the asymmetric case does not.) However, real materials do not necessarily have particle-hole symmetry and it is generally believed that they are more likely to be in the mixed-valence regime. Varma has argued that charge fluctuations are crucial to the understanding of the physics of these systems.[8] He points out that such fluctuations should reduce the magnetic correlations between sites. As we shall see in Sec. IV B, this is confirmed by our calculations. Indeed neutron-scattering experiments have indicated the absence of magnetic correlations in CeNiSn.[9] In addition, measurements of the occupation of the f orbital in $Ce_3Bi_4Pt_3$ give $n_f = 0.865$ at $T = 0$,[10] indicating a mixed-valence state. Thus it is important to determine the properties of the asymmetric Anderson lattice in the mixed-valence regime.

Previous studies of the mixed-valence case have been hampered by various limitations. Analytic calculations, which include the Gutzwiller approach[11,12] and the slave boson mean-field approximation,[13,14] do not distinguish between the different kinds of gaps (spin, charge, and quasiparticle gaps). Numerical approaches have been limited to four-site chains[15,16] and did not consider the charge gap.[15]

In this paper we present a systematic study of all three gaps of the half-filled Anderson lattice in both the Kondo and the mixed-valence regime. The staggered susceptibility $\chi(q=2k_F)$, the f-spin–f-spin correlation functions, and the occupation n_f of the localized orbital have been calculated for the mixed-valence case.

The density-matrix renormalization-group technique allows us to consider chains of up to 24 sites. This gives us an advantage over other numerical approaches,[5,15,16] which can only deal with short chains. Not only are we able to get f-spin–f-spin correlation functions, but by considering long chains, we can also study the behavior of the f-spin–f-spin correlations in both regimes. We establish that the amplitude of the correlations decays exponentially in space and we can calculate the correlation length as a function of the parameters. Previous Monte Carlo studies of the symmetric case were unable to distin-

0163-1829/95/51(16)/10301(12)/$06.00

guish between power law or exponential behavior[5] because of the length of the lattice. In the mixed-valence case, where the accuracy is higher than for the symmetric case at large U, we can get the extrapolated value of the spin gap and the average occupation of the localized orbital for infinite chains. We find that both have power-law behavior for large U. This analysis was not possible in previous studies of short chains.[15,16]

We also consider the $U=\infty$ in which the doubly occupied states of the localized orbital are suppressed. Several approximation schemes, such as the Gutzwiller technique and the slave boson mean-field approach, have been applied in this limit. However, it is not clear how well these approximations describe the properties of the Anderson Hamiltonian. To find out, we compare some of our results with those of the slave boson mean-field approach. We find good agreement when the system is in the mixed-valence regime, but as the system approaches the Kondo regime, the slave boson picture breaks down.

The paper is organized as follows. We consider the one-dimensional Anderson lattice at half filling using the density-matrix formulation of the quantum renormalization-group technique,[17,18] which is briefly described in Sec. II. After discussing the Anderson and Kondo lattice Hamiltonians in Sec. III, we give our results in Sec. IV. In both the symmetric and the asymmetric case, we find in Sec. IV A that the charge gap is larger than the spin gap. In Sec. IV B we study the Ruderman-Kittel-Kasuya-Yosida (RKKY) interactions by calculating the f-spin–f-spin correlation function and the staggered susceptibility $\chi(q=2k_F)$ as a function of U. Our results show that in the Kondo regime the RKKY interactions become important as U increases, while in the mixed-valence case such magnetic correlations are suppressed because the f orbitals are not always occupied. In Sec. IV C we find that the occupation of n_f of the localized orbital changes from 1 at $U=0$ to a value close to 0.7 at $U=\infty$ in the asymmetric case when the localized band is at the Fermi energy. (In the symmetric case $n_f=1$.) In Sec. IV D we study the $U=\infty$ case. We present our conclusions in Sec. V.

II. QUANTUM RENORMALIZATION-GROUP TECHNIQUE

The density-matrix formulation of the numerical renormalization group has proven extremely useful for the study of the ground-state and low-energy excitations of one-dimensional systems.[19,20] It has distinct advantages over other computational techniques. For example, it allows us to study chains longer than what is achievable by exact diagonalization and it avoids the problem of Monte Carlo calculations where very low temperatures are difficult to attain.

In real-space renormalization-group schemes, the system is divided into small blocks. The traditional renormalization-group approach consists of diagonalizing the Hamiltonian of a small block, keeping the lowest-energy eigenstates, and then forming a bigger block by combining a few of the small blocks. The drawback of this approach is that it completely neglects quantum fluctuations at the boundary of the blocks. For this reason, the standard approach performs poorly and is not significantly improved by increasing the number of states kept.[17]

The density-matrix formulation of the renormalization group provides a systematic method of choosing the states to keep for the bigger block and at the same time it takes into account the quantum fluctuations at the boundaries. The procedure for a one-dimensional lattice goes as follows. We divide the chain into four blocks. Typically, blocks 1 and 4 have many sites and blocks 2 and 3 (in the center of the chain) are single sites. We find the ground state of the Hamiltonian for the lattice:

$$|\psi\rangle=\sum_{i1,i2,i3,i4}\psi_{i1,i2,i3,i4}|i1,i2,i3,i4\rangle\ , \tag{1}$$

where $i1$, $i2$, $i3$, and $i4$ label states in blocks 1, 2, 3, and 4. Then we consider blocks 1 and 2 to be the "system" and the rest of the chain to be the "environment." The objective is to construct a new block 1 out of blocks 1 and 2 by keeping only a fraction of the total number of states. In order to choose which states to keep, we form the density matrix for blocks 1 and 2 by tracing out the degrees of freedom of blocks 3 and 4:[21]

$$\rho(i1,i2,ii1,ii2)=\sum_{i3,i4}\psi_{i1,i2,i3,i4}\cdot\psi^{*}_{ii1,ii2,i3,i4}\ . \tag{2}$$

We then diagonalize this density matrix. The eigenvalues of the density matrix give the weight of the associated eigenstates.[21] Since it is not possible to keep all the states, we truncate the basis by keeping a predetermined number of states with the largest weights. We use these eigenstates to construct the basis of the new block 1, which is made out of the old blocks 1 and 2. In this way, we increase the size of block 1 by one site.

It is possible to target more than just the ground state; the lowest excited states can be calculated as well by simply diagonalizing the Hamiltonian for these states. In each case the diagonalization is performed in a subspace with fixed quantum numbers, e.g., with a fixed number of electrons and a fixed z component of the total spin. This method performs at its best for open boundary conditions in which there is no hopping past the ends of the chain. We typically keep 100 states, although for cases where higher accuracy is needed, we keep up to 200 states. For small values of the Coulomb repulsion, the results are very accurate with truncation errors of the order of 10^{-8}, while for large values of the Coulomb repulsion the accuracy is reduced and the truncation errors increase to 10^{-4}. For a more detailed description of the method, see Ref. 17.

As a check for our method, we compare our energies and correlation functions with exact diagonalization results. For short chains we can keep all the states and we obtain full agreement with exact diagonalization. As another check, we compare the ground-state energy for the symmetric Anderson lattice with Gutzwiller[22] and Monte Carlo results[7] as shown in Fig. 1. We plot $(e_0+U/2)/|e_0|$, where e_0 is the ground-state energy per site. The Monte Carlo simulations calculated the

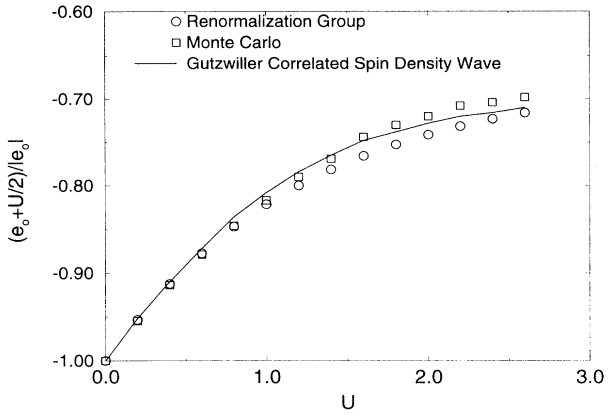

FIG. 1. $(e_0+U/2)/|e_0|$ vs U for the symmetric Anderson lattice with $V/2t=0.375$. e_0 is the ground-state energy per site. Our results are in good agreement with the Gutzwiller (Ref. 22) and Monte Carlo (Ref. 7) results.

ground-state energy for 16 site chains with periodic boundary conditions.[7] We use open boundary conditions and chains of 24 sites. The Gutzwiller values are for a correlated spin-density wave.[22] We obtain good agreement with both calculations. For large U, our energies lie below the Monte Carlo and the Gutzwiller values, giving a better upper bound for the ground-state energy. In this regime the binding energy is proportional to $1/U$, in agreement with perturbation theory.

III. THE PERIODIC ANDERSON HAMILTONIAN

We consider the standard periodic Anderson Hamiltonian in one dimension:

$$H=-t\sum_{i,\sigma}(c_{i\sigma}^{\dagger}c_{i+1\sigma}+c_{i+1\sigma}^{\dagger}c_{i\sigma})+\epsilon_f\sum_{i,\sigma}n_{i\sigma}^{f}+U\sum_{i}n_{i\uparrow}^{f}n_{i\downarrow}^{f}+V\sum_{i,\sigma}(c_{i\sigma}^{\dagger}f_{i\sigma}+f_{i\sigma}^{\dagger}c_{i\sigma}) , \quad (3)$$

where $c_{i\sigma}^{\dagger}$ and $c_{i\sigma}$ create and annihilate conduction electrons with spin σ at lattice site i, $f_{i\sigma}^{\dagger}$ and $f_{i\sigma}$ create and annihilate local f electrons, t is the hopping matrix element for conduction electrons between neighboring sites, ϵ_f is the energy of the localized f orbital, U is the on-site Coulomb repulsion of the f electrons, and V is the on-site hybridization matrix element between electrons in the f orbitals and the conduction band. For simplicity we neglect orbital degeneracy. U, V, t, and ϵ_f are taken to be real numbers.

Let us examine the Anderson Hamiltonian in various limits. For $U=0$ this Hamiltonian can be exactly diagonalized in k space. We obtain two hybridized bands with energies $\lambda_k^{\pm}$:

$$\lambda_k^{\pm}=\tfrac{1}{2}\{[\epsilon_f-2t\cos(ka)]\pm\sqrt{[\epsilon_f+2t\cos(ka)]^2+4V^2}\} , \quad (4)$$

where a is the lattice constant. When there are two electrons per unit cell, the lower band is full while the upper one is empty. Thus the system is insulating when $N_e=2L$. Here N_e is the number of electrons and L is the number of sites in the lattice.

When the mixing term is small [$\pi V^2/2t(\epsilon_f+U)\ll 1$ and $\pi V^2/2t\epsilon_f\ll 1$], the Anderson Hamiltonian can be mapped into the Kondo model[23]

$$H_K=-t\sum_{i,\sigma}(c_{i\sigma}^{\dagger}c_{i+1\sigma}+c_{i+1\sigma}^{\dagger}c_{i\sigma})+J_{\rm eff}\sum_{i}\mathbf{S}_i^f\cdot\mathbf{s}_i^c , \quad (5)$$

where $\mathbf{s}_i^c$ is the spin density of the conduction electrons at site i and $J_{\rm eff}$ is given by the Schrieffer-Wolff transformation[23]

$$J_{\rm eff}=-\frac{2|V|^2U}{\epsilon_f(\epsilon_f+U)} . \quad (6)$$

Note that for the symmetric case, where $\epsilon_f=-U/2$, $J_{\rm eff}=8V^2/U$, and for $U=\infty$, $J_{\rm eff}=-2V^2/\epsilon_f$.

Although there is no direct interaction between the f electrons in the Hamiltonian (3), there is an indirect exchange coupling between the f sites via the conduction band. This is the RKKY coupling, originally derived for the magnetic interaction between nuclei in metals.[24] An electron in the f orbital tends to polarize the spin of the conduction electron cloud around it. The spin of the conduction electron polarization cloud oscillates with distance and it polarizes the spin of the f electrons at neighboring sites. In the case of the Anderson Hamiltonian, the RKKY coupling constant can be obtained by considering two Anderson impurities in a gas of conduction electrons. The hybridization term is taken as a perturbation and the fourth-order contribution to the perturbation expansion gives the coupling between sites. The effective Hamiltonian for the two impurities is

$$H_{\rm RKKY}=J_{\rm RKKY}\mathbf{S}_1^f\cdot\mathbf{S}_2^f , \quad (7)$$

where $\mathbf{S}_1^f$ and $\mathbf{S}_2^f$ are the spin operators for the f electrons on the two impurities. The explicit expression for $J_{\rm RKKY}$ is fairly complicated in general,[5] but it can be shown that it favors antiferromagnetic alignment of the f spins with wave vector $q=2k_F$, where k_F is the Fermi wave vector of the noninteracting conduction electrons.

For the one-dimensional asymmetric case ($\epsilon_f=-U/2$) at half filling, $2k_Fa=\pi$ and the asymptotic expression for large distances is[5]

$$J_{\rm RKKY}=\left[\frac{8V^2}{U}\right]^2\frac{1}{8\pi t}\frac{(-1)^l}{l} , \quad (8)$$

where l is the distance between $\mathbf{S}_1$ and $\mathbf{S}_2$ in units of the lattice constant. Note that $J_{\rm RKKY}=(-1)^lJ_{\rm eff}^2/8\pi tl$, that is, the Kondo coupling constant is the parameter that governs the f-f correlations in the Kondo regime. The asymptotic expression (8) is the same as the one obtained by starting with the Kondo Hamiltonian and doing second-order perturbation theory in $J_{\rm eff}$.

We expect RKKY interactions to be important in the Kondo regime where the occupancy of the f orbital is very close to 1. In the mixed-valence regime, the occu-

pancy of the f level is reduced and therefore RKKY correlations should be suppressed.[8]

A. Symmetric case

The symmetric case corresponds to a value of $\epsilon_f=-U/2$. For large U, the f level lies well below the Fermi surface and the system is in the Kondo regime. Particle-hole symmetry ensures that the occupancy of the f level, n_f, is always one. In the strong-coupling regime ($8V^2/U \ll t$), charge fluctuations in the f orbital are highly suppressed because the Coulomb repulsion makes the states with one electron in the f level much more energetically favorable than the state with two electrons or the state with the orbital empty.

In addition to the usual SU(2) spin symmetry, this particular choice of ϵ_f introduces an SU(2) charge pseudospin symmetry into the system.[6] The pseudospin operator (**I**) can be obtained from the spin operator **S** by performing a particle-hole transformation on one of the spin species.[6] Its components are

$$\begin{aligned} I_z &= \tfrac{1}{2}\sum_i (c_{i\uparrow}^\dagger c_{i\uparrow}+c_{i\downarrow}^\dagger c_{i\downarrow}+f_{i\uparrow}^\dagger f_{i\uparrow}+f_{i\downarrow}^\dagger f_{i\downarrow}-2)\ , \\ I_+ &= \sum_i (-1)^i (c_{i\uparrow}^\dagger c_{i\downarrow}^\dagger - f_{i\uparrow}^\dagger f_{i\downarrow}^\dagger)\ , \\ I_- &= \sum_i (-1)^i (c_{i\downarrow} c_{i\uparrow} - f_{i\downarrow} f_{i\uparrow})\ . \end{aligned} \tag{9}$$

The z component of the pseudospin is equal to $(N_{\rm el}/2)-L$. Note that half filling corresponds to $I_z=0$. An $I_z=1$ state can be achieved by adding two electrons.

All the energy eigenstates of the symmetric Anderson model have a definite value of S and I. At half filling the ground state is a singlet both in spin and pseudospin space ($S=0, I=0$).[25] The lowest-lying excited state is a spin triplet. The energy difference between these two states is the spin gap Δ_s:

$$\Delta_s = E(S=1,I=0)-E_0(S=0,I=0)\ , \tag{10}$$

where E_0 is the energy of the ground state.

To find the charge gap, we note that optical experiments measure the charge gap by measuring the conductivity, which is determined by the current-current correlation function. The current is related to the charge density through the continuity equation. Thus the lowest-lying charge excitation is the lowest excited state $|n\rangle$ with $S=0$ such that $\langle 0|\sum_q \rho_q|n\rangle \neq 0$, where ρ_q is the q component of the Fourier transformed charge-density operator and $|0\rangle$ is the ground state.[26] Notice that ρ_q is related to $\mathbf{I}_q^z$, where $\mathbf{I}_q$ is a Fourier-transformed vector in pseudospin space given by

$$\begin{aligned} I_q^z &= \tfrac{1}{2}\sum_i e^{-i\mathbf{q}\cdot\mathbf{r}_i}(c_{i\uparrow}^\dagger c_{i\uparrow}+c_{i\downarrow}^\dagger c_{i\downarrow}+f_{i\uparrow}^\dagger f_{i\uparrow}+f_{i\downarrow}^\dagger f_{i\downarrow}-2)\ , \\ I_q^+ &= \sum_i e^{-i\mathbf{q}\cdot\mathbf{r}_i}(-1)^i(c_{i\uparrow}^\dagger c_{i\downarrow}^\dagger - f_{i\uparrow}^\dagger f_{i\downarrow}^\dagger)\ , \\ I_q^- &= \sum_i e^{-i\mathbf{q}\cdot\mathbf{r}_i}(-1)^i(c_{i\downarrow} c_{i\uparrow} - f_{i\downarrow} f_{i\uparrow})\ . \end{aligned} \tag{11}$$

Using the Wigner-Eckart theorem, one can show that the $(I=1,S=0)$ states are the only states $|n\rangle$ for which the charge density ρ_q has finite matrix elements $\langle n|\rho_q|0\rangle$ with the ground state $|0\rangle$. Thus the charge gap Δ_c is the energy difference between the ground state and the lowest pseudospin triplet state[6]

$$\Delta_c = E(S=0,I=1)-E_0(S=0,I=0)\ . \tag{12}$$

The quasiparticle gap gives the energy for making a noninteracting particle and hole. It is defined as

$$\Delta_{\rm qp}=E_0(N_e=2L+1)+E_0(N_e=2L-1)-2E_0(N_e=2L). \tag{13}$$

Due to the particle-hole symmetry of the symmetric case, one can write

$$\Delta_{\rm qp}=2[E_0(N_e=2L+1)-E_0(N_e=2L)]\ . \tag{14}$$

The quasiparticle gap can be thought of as the difference of chemical potentials

$$\Delta_{\rm qp}=\mu_{N+1}-\mu_N\ , \tag{15}$$

where $\mu_N=E_0(N_e)-E_0(N_e-1)$ and $N_e=2L$ for half filling.

For $U=0$, all the gaps coincide and are given by the hybridization gap:

$$\Delta_s=\Delta_c=\Delta_{\rm qp}=\lambda_0^+-\lambda_\pi^-=2\sqrt{t^2+V^2}-2t\ . \tag{16}$$

As $U\to\infty$, the f electrons decouple from the conduction electrons and all the gaps go to zero.

We can also define the gap $\Delta_{\rm ns}$ between the ground state and the lowest excited neutral singlet state, which has quantum numbers $(S=0,I=0)$.[4] For the half-filled Kondo lattice, the neutral singlet has been found to be an elementary excitation consisting of a particle and a hole, which are $(S=\frac{1}{2},I=\frac{1}{2})$ excitations. In a single-site basis, a hole is a site with one f electron and no conduction electrons with quantum numbers $(S=\frac{1}{2},I=\frac{1}{2},I_z=-\frac{1}{2})$, while a particle is a site with one f electron and two conduction electrons with $(S=\frac{1}{2},I=\frac{1}{2},I_z=+\frac{1}{2})$. The Kondo and Anderson lattices agree for small $J_{\rm eff}/t$. In this regime the neutral singlet gap is smaller than the charge and the quasiparticle gaps, but larger than the spin gap.[4] However, for small U, the lowest-lying $(S=0,I=0)$ excited state is not an elementary excitation, but presumably consists of two spin excitations. Indeed, for $U=0$, one can show that $\Delta_{\rm ns}=2\Delta_s$. In the small-$U$ limit, there are bands of spin and charge excitations that lie between the lowest excited neutral singlet state and the ground state. Because of this, it is hard for the numerical-renormalization-group technique to accurately calculate the energy of the neutral singlet state for small U. For this reason, we have not calculated the neutral singlet gap.

B. Asymmetric case

The symmetric case is typically studied in the strong-coupling regime ($8V^2/U \ll t$) where the f level lies far below the Fermi energy. However, in real materials the f

level can be near the Fermi surface even though U is large. In addition, real materials ordinarily do not have particle-hole symmetry. For this reason we consider the asymmetric case in which ϵ_f can have any value irrespective of U. In particular, we place the f orbital right at the Fermi level ($\epsilon_f=0$) so that states with no electrons and states with one electron in the f level are equal in energy, while states with two electrons are highly suppressed due to the strong Coulomb repulsion. In this mixed-valence case, charge fluctuations are allowed and the occupation of the f level, n_f, is always less than one for $U>0$.

Note that there is no particle-hole symmetry and the pseudospin operator is no longer conserved. Only the total number of electrons (I_z) remains a good quantum number. For all the values of the parameters that we explored, we found that the ground state is still a spin singlet at a half filling. There is still a gap to the lowest-lying excited state, which is a spin triplet. Thus the spin gap can still be defined as

$$\Delta_s=E(S=1)-E_0(S=0)\ . \tag{17}$$

The quasiparticle gap is defined in Eq. (13). Note that in this case $E(2L+1)\neq E(2L-1)$ since there is no particle-hole symmetry.

Unlike the symmetric case we can no longer use charge pseudospin symmetry to find the charge gap. We must use the fact that the lowest-lying charge excitation is the lowest excited state $|n\rangle$ with $S=0$ such that $\langle n|\sum_q \rho_q|0\rangle\neq 0$, where ρ_q is the q component of the Fourier transformed charge-density operator and $|0\rangle$ is the ground state.[26] Using the fact that $\sum_q \rho_q = c^{\dagger}_{i=0}c_{i=0}$, we find that $|n\rangle$ is the lowest $S=0$ excited state. Let its energy be denoted by $E_1(S=0)$. Then the charge gap is given by

$$\Delta_c=E_1(S=0)-E_0(S=0)\ . \tag{18}$$

IV. RESULTS

In using the density-matrix renormalization-group technique, we consider lattices up to 24 sites long and we use open boundary conditions. We set $t=1$ so that energies are measured in units of t. For the symmetric case, by definition, $\epsilon_f=-U/2$. In order to study the asymmetric case in the mixed-valence regime, we set $\epsilon_f=0$, that is, ϵ_f is at the Fermi energy. We fix $V=1$ and vary U from 0 to 30. Although this value of V is somewhat larger than in real materials, it is convenient for numerical reasons and for comparison with previous calculations.[6]

A. Gaps

In Figs. 2(a) and 2(b), we plot the gaps versus U for different chain sizes for the symmetric and asymmetric cases, respectively.

Relative gap sizes. In both the symmetric and asymmetric cases, the charge and quasiparticle gaps are larger than the spin gap for $U>0$. This is consistent with experiments that find that the charge gap is larger than the spin gap in $Ce_3Bi_4Pt_3$.[28] As we shall see, in the mixed-valence case the ratio $\Delta_c/\Delta_s\sim 2$ for large U. This agrees with the experimental value of 1.8 for $Ce_3Bi_4Pt_3$.[28] In the Kondo regime, one expects a much larger ratio when U is large; in fact, this ratio diverges in the symmetric case as $U\rightarrow\infty$.[6]

Note that the gaps have a smaller value at $U=\infty$ than at $U=0$. In the asymmetric case this reduction is not as large as in the symmetric case. This decrease is due to many-body interaction effects and may explain why band-structure calculations[29,30] find a larger gap than the optical gap measured experimentally.[31]

Nature of the excitations. For the symmetric case [Fig. 2(a)], notice that the spin gap decreases monotonically with increasing U. In contrast to the monotonic behavior of the spin gap, Fig. 2(a) shows that the charge and quasiparticle gaps initially increase with U, go through a maximum, and then decrease. This behavior was also observed by Steiner *et al.*[27] To understand this, note that the quasiparticle gap is obtained by adding a particle to

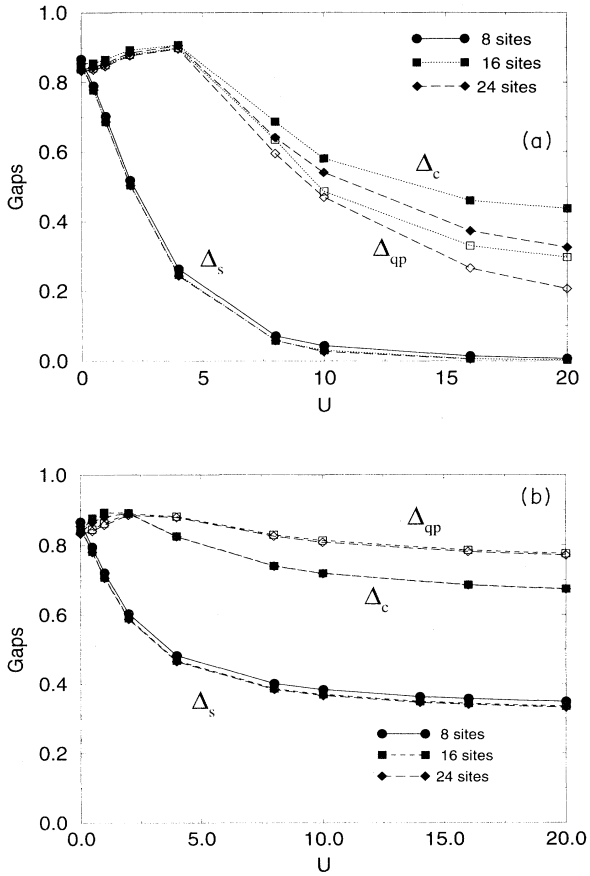

FIG. 2. (a) Gaps vs U for the symmetric case ($t=1, V=1, \epsilon_f=-U/2$). Open symbols are for the quasiparticle gap. Filled symbols are for the spin gap and the charge gap. Note that $\Delta_s<\Delta_{qp}<\Delta_c$ for $U>0$. (b) Gaps vs U for the asymmetric case ($t=1, V=1, \epsilon_f=0$). The charge and the quasiparticle gap cross at $U\sim 2$. Note that the spin gap is smaller than both of them.

the system. For very small U, this particle goes predominantly into an f orbital; so as U increases, the gap also increases due to the Coulomb repulsion. However, for large U, the extra particle goes mostly into the conduction band and the gap starts decreasing. One can see how much of an additional particle goes into an f orbital by plotting $\langle N_f \rangle - L$ vs U for the state with $N_{\rm el} = 2L+1$ (see Fig. 3). Since the total number of f electrons N_f equals L at half filling with particle-hole symmetry, $\langle N_f \rangle - L$ tells us how much of the extra particle is in the f orbital. One can see in Fig. 3 that the extra particle goes mainly into an f level for small U but, as U increases, it goes more and more into the conduction band.

Now we discuss the charge gap shown in Fig. 2(a). In the symmetric case, the charge gap is obtained by adding two particles to the half-filled system to get an $(I=1, I_z=1)$ state. It has a maximum as a function of U for the same reason that the quasiparticle gap does. The fact that $\Delta_c > \Delta_{\rm qp}$ for any finite value of U means that the two extra particles repel each other. So as $L \to \infty$, they will be infinitely apart and Δ_c will equal $\Delta_{\rm qp}$.

In Fig. 2(b) we show the gaps versus U in the asymmetric case. We see that for $U \lesssim 2$, Δ_c is greater than $\Delta_{\rm qp}$, but as U increases, they cross. This crossover can be interpreted as follows. The quasiparticle gap consists of two noninteracting $S=\frac{1}{2}$ excitations. The charge gap, on the other hand, is given by the lowest $S=0$ excited state. For small U this state consists of two $S=\frac{1}{2}$ excitations, while for large U there is a crossover to a state made out of two $S=1$ excitations. This picture is supported by the fact that for small U, $\Delta_c \sim \Delta_{\rm qp}$, but as U increases, $\Delta_c \sim 2\Delta_s$.

Finite-size effects as $U \to \infty$. As $U \to \infty$ in the symmetric case, the conduction electrons and the f electrons decouple and the gaps approach their values for a free-electron band on a finite-size lattice with open boundary conditions. We confirmed this by calculating the gaps on finite-size lattices for free electrons. The charge and quasiparticle gaps have large finite-size effects, especially for large U. Nishino and Ueda[6] find a much smaller charge gap in the large-U limit because they use periodic boundary conditions and the charge gap goes to zero for free electrons on a ring. On the other hand, our values for the spin gap agree with the results of Nishino and Ueda[6] because the spin gap has small finite-size effects. To understand this, note that the spin excitation has small dispersion because it is a spin flip that has mainly f character. This makes it a local excitation, which is not very sensitive to the length of the lattice or to the boundary conditions. To confirm this picture, in Fig. 3 we plot $\langle S_z^f \rangle$ versus U for the excited $(S=1, I=0, S_z=1)$ state. (Here S_z^f refers to the z component of the total f spin of the chain.) For $U=0$, $\langle S_z^f \rangle$ is about 80% of the total spin and it gets very close to 100% for larger U.

In the asymmetric case, the gaps tend to a finite value[15] as $U \to \infty$. The fact that the gaps are finite is not a finite-size effect but rather can be understood in the following way. For $U=\infty$, states with double f occupancy are suppressed, but the proximity of the f level to the Fermi energy allows the system to fluctuate between states with no f electrons in the local orbital and states with one f electron. This leads to hybridization and the formation of the gap. Another way to see that there is hybridization is to recall from Eq. (6) that $J_{\rm eff} = -2V^2/\epsilon_f$ for $U=\infty$. The presence of a finite $J_{\rm eff}$ leads to hybridization and gap formation.

Spin gap. For the asymmetric case, we can study how the spin gap approaches its $U=\infty$ value. We begin by extrapolating the spin gap to its value at $L \to \infty$ in the following way: for each value of U, we plot Δ_s versus $1/L^2$ and obtain a straight line (Fig. 4). The intercept is then the value for $L \to \infty$. To understand why the spin gap is proportional to $1/L^2$, note that the spin density versus site for the $(S=1, S_z=1)$ state is shaped like a particle-in-a-box wave function of wavelength $\sim L$. This

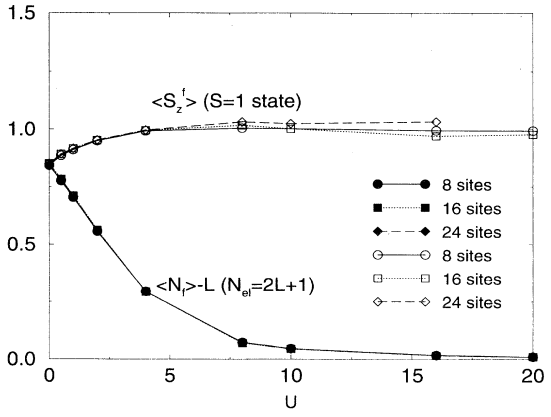

FIG. 3. Character of the spin and quasiparticle excitations vs U. The open symbols are for $\langle S_z^f \rangle$ in the lowest excited $S=1$ state at half filling. The filled symbols are for $\langle N_f \rangle - L$ in the ground state with $2L+1$ electrons. The spin excitations have mainly f character while the particle excitations have the character of conduction electrons in the strong-coupling regime.

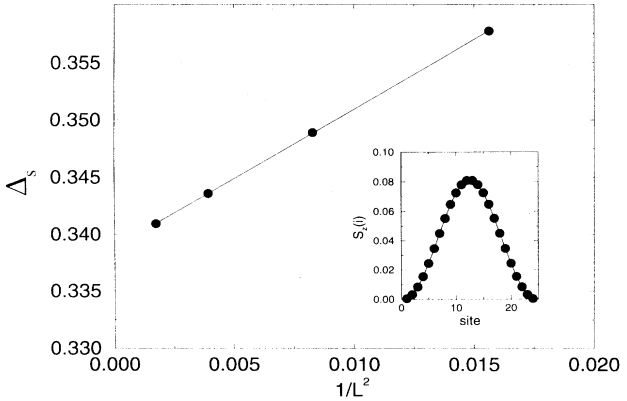

FIG. 4. Spin gap vs $1/L^2$ in the asymmetric case $(t=1, V=1, \epsilon_f=0, U=16)$. The intercept of the linear fitting gives the $L=\infty$ value. Inset: S_z on a site vs the site for the lowest excited $(S=1, S_z=1)$ state on a 24-site lattice at half filling.

is shown in the inset of Fig. 4. We then interpret the spin gap as the kinetic energy of the quasiparticle, which is proportional to the square of the wave vector and goes as $1/L^2$.

We study the behavior of the spin gap for $L \to \infty$ and we find that, for large U with $\epsilon_f = 0$ in the asymmetric case, it can be fitted by the form

$$\Delta_s(U) = \Delta_s(U=\infty) + \frac{\text{const}}{U^\alpha} \tag{19}$$

with $\alpha \to 1$ as $U \to \infty$. For $\epsilon_f < 0$, a study of the large-U behavior of the gap for short chains suggest that the spin gap approaches a finite value as $(\epsilon_f + U)^{-1}$ for the asymmetric case.

B. RKKY interactions

We study RKKY interactions between f spins in the ground state by calculating the f-spin–f-spin correlation function and the staggered susceptibility. We first turn our attention to the correlation function.

1. f-spin–f-spin correlations

We study the f-spin–f-spin correlations in the ground state due to RKKY interactions. In Fig. 5 we show the spin-spin correlation function of the f electrons as a function of spatial separation r (measured in units of the lattice constant) for different values of U. Figure 5(a) corresponds to the symmetric case and Fig. 5(b) to the asymmetric case.

Mixed-valence case. In the mixed-valence case, the RKKY correlations are highly suppressed because the f orbital is not always occupied. This can be seen in the f-spin–f-spin correlation function shown in Fig. 5(b). In contrast to the symmetric case, we see that the increase of U by an order of magnitude does not change the rapid decrease of the correlations with distance.

It is tempting to speculate that another reason why the RKKY correlations are suppressed is that the effective Kondo coupling J_{eff} becomes very large as ϵ_f approaches the Fermi level. (Recall that $J_{\text{eff}} = -2V^2/\epsilon_f$ for $U = \infty$.) In the Kondo lattice model, RKKY correlations decrease with increasing J_{eff}. The problem with this explanation is that the Schrieffer-Wolff transformation is no longer valid when $|\epsilon_f| \ll \Gamma$ where $\Gamma = \pi V^2 \rho$. Even with more sophisticated techniques,[33] there is no known analytic expression for J_{eff} when $|\epsilon_f| \ll \Gamma$ and $\Gamma/U \ll 1$.

Symmetric case. For the symmetric case we see that as we increase U from 2 to 20, the amplitude of the oscillations becomes much larger and persists for longer distances. There are several ways to understand why RKKY interactions increase with large U. First one notes that as U increases, the effective Kondo coupling constant $J_{\text{eff}} = 8V^2/U$ decreases relative to the hopping matrix element t. Increased hopping means increased correlations between sites. The decrease of the gaps also enhances RKKY interactions. Another way to understand the growth of RKKY interactions is to note that the Kondo temperature $T_K \sim \exp(-1/\rho J_{\text{eff}})$ decreases with increasing U and, as a result, the Kondo compensation cloud increases in size. Uncompensated f spins within the cloud develop correlations.[5] A third way to view this was suggested by Varma and Doniach.[32] In the Kondo model they have argued that RKKY interactions will dominate as J_{eff} decreases because the RKKY energy scale goes as J_{eff}^2 while the Kondo energy sale depends exponentially on J_{eff}. Opposing this enhancement of RKKY interactions is the fact that the effective RKKY coupling will decrease as J_{eff} decreases, but only as J_{eff}^2.

We find that the amplitude of the RKKY oscillations decrease exponentially with distance and it can be fitted by $\exp(-r/\xi)$, where ξ is the correlation length. In Fig. 6 we show the behavior of the correlation length for the symmetric case as a function of the effective Kondo coupling constant $J_{\text{eff}} = 8V^2/U$. We plot two different sets of parameters and we see that the curves lie on top of each other, confirming the fact that the relevant parameter in the strong-coupling regime is J_{eff}. We also show the results for the one-dimensional Kondo chain, which agree

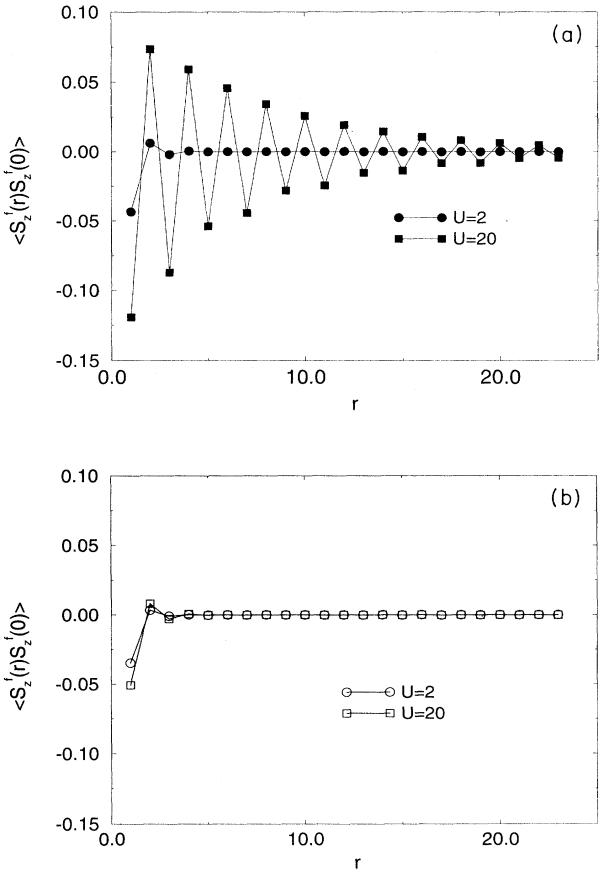

FIG. 5. (a) f-spin–f-spin correlation function versus distance r apart for the symmetric case ($t=1, V=1, \epsilon_f = -U/2, L=24$). The oscillations increase in amplitude and persist for longer distances as U increases from 2 to 20. (b) f-spin–f-spin correlation function versus distance r apart for the asymmetric case ($t=1, V=1, \epsilon_f = 0, L=24$). As U increases from 2 to 20, neither the amplitude of the oscillations nor the correlation length change significantly.

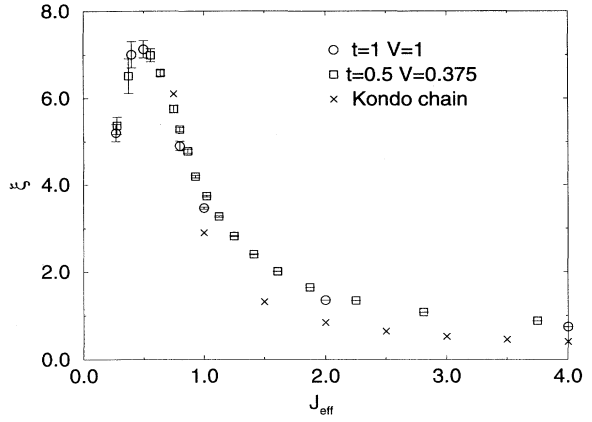

FIG. 6. Correlation length vs $J_{\text{eff}}=8V^2/U$ in the symmetric case. The curves for different sets of parameters fall on top of each other for $J_{\text{eff}}<1$. The data for the Kondo chain are taken from Ref. 36. All data are for $L=24$.

very well for small J_{eff}. As J_{eff} decreases (i.e., as U increases), the correlation length goes up to a maximum and then starts going down. There are two ways to interpret this. One view says that this is to be expected since the f electrons decouple from the conduction electrons as J_{eff} goes to zero and the correlations between different sites decreases. On the other hand, one can interpret the exponential decay of the spin correlations with distance as a consequence of the existence of a gap in the excitation spectrum. The gap suppresses low-energy (long-wavelength) magnetic excitations and this greatly reduces long-range correlations. As the gap decreases, one would expect the correlation length to monotonically increase roughly as $\xi\sim v_{\text{Fermi}}/\Delta_S$.[14] Since we find a maximum in ξ, our data support the first point of view, although the error bars on ξ are bigger for small J_{eff} because in this regime the effects of the ends affect the wave function of the entire lattice. This can be seen, for example, in the oscillations of the hybridization energy from site to site. When J_{eff} is small, these oscillations remain sizable even in the center of the lattice. For large J_{eff}, these oscillations decrease rapidly as one goes away from the ends of the chain.

2. *Staggered susceptibility*

In order to further study the magnetic properties of the system, we calculate the staggered susceptibility $\chi(q)$ as a function of the momentum q. To calculate $\chi(q)$, we apply a small magnetic field $h=h_0\cos(qr)$ in the z direction for different values of h_0 and plot $S(q)$ versus h_0. $S(q)$ is the Fourier transform of $\langle 0|S_z(i)|0\rangle$. (The field couples to both the f spins and the conduction spins.) If h_0 is small enough, this plot is a straight line whose slope is the susceptibility. For this application, q has to be a good quantum number. Therefore we use periodic boundary conditions. This greatly reduces the accuracy of the method and we can only study short chains (four or six sites).

In Fig. 7 we plot the staggered susceptibility $\chi(qa=2k_Fa=\pi)$ versus U. We see that in the symmetric case the staggered susceptibility diverges as $U\rightarrow\infty$. This is consistent with the growth of RKKY oscillations. In addition, as $U\rightarrow\infty$, the f electrons decouple from the conduction electrons and become polarized in an arbitrarily small magnetic field. As a result, the susceptibility will diverge for all q. In contrast, in the mixed valence case, as $U\rightarrow\infty$, the staggered susceptibility $\chi(q=2k_F)$ approaches a finite value $\chi(U=\infty)$. $\chi(U)$ does not change much with U because of the reduction of the magnetic correlations in the mixed-valence regime.

In the inset of Fig. 7 we show $\chi(q)$ versus q for both the symmetric and asymmetric cases. In the asymmetric case the peak at $q=2k_F$ is greatly reduced, that is, $\chi(q)$ shows little structure. This is consistent with neutron-scattering results on CeNiSn,[9] in which they find that $\chi(q)$ is independent of q within experimental error. In fact the fluctuations we find in $\chi(q)$ are an order of magnitude smaller than those seen experimentally, though one should keep in mind that our lattices are small and the values we chose for the parameters are not necessarily appropriate for CeNiSn.

In the mixed-valence regime the occupation of the f level is less than 1 per site, which implies that the conduction electron occupation is greater than 1 per site. One might worry that this implies that the RKKY wave vector $2k_F$ is no longer equal to π, but rather is equal to a wave vector that is incommensurate with the lattice. Could this explain the lack of divergence for $\chi(qa=\pi)$ seen in Fig. 7? The answer is no. The suppression of RKKY correlations can clearly be seen in Fig. 5(b). Since Fig. 5(b) is in real space, any RKKY correlations, even those with an incommensurate wave vector, would show up in this plot.

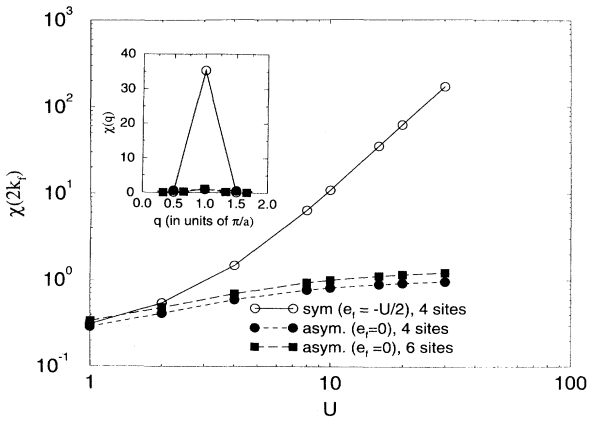

FIG. 7. Staggered susceptibility vs U for short chains with periodic boundary conditions ($t=1, V=1$). In the asymmetric case the susceptibility shows little change with U due to the suppression of the magnetic correlations in the ground state. Inset: staggered susceptibility vs q for short chains with $U=16$. Notice that the asymmetric case (filled symbols) shows little dispersion, indicating again that RKKY interactions are suppressed in the asymmetric case.

C. Occupancy of the f level

In the symmetric case, the occupation of the f level is 1 in the ground state due to particle-hole symmetry. However, in the asymmetric case we expect the f-level occupation n_f to be less than 1 in the mixed-valence regime. We can calculate the f-level occupation n_f per site by taking the expectation value of n_{fi} on each site with respect to the ground-state wave function and then averaging over the sites. Thus n_f is given by

$$n_f=\frac{1}{L}\sum_{i,\sigma}\langle 0|f_{i\sigma}^{\dagger}f_{i\sigma}|0\rangle\ , \tag{20}$$

where $|0\rangle$ is the ground state. In Fig. 8 we plot $n_f(L=\infty)$ versus U. We can extrapolate to infinite lengths because n_f versus $1/L$ follows a straight line due to the factor of $1/L$ in Eq. (20).[34] We see that as U increases, n_f decreases from 1 towards a value close to 0.7, indicating a mixed-valence state at large U. For large U, n_f follows power-law behavior:

$$n_f(U)=n_f(U=\infty)+\frac{\text{const}}{U^{\beta}}\ , \tag{21}$$

where $n_f(U=\infty)=0.685\pm0.001$ and β goes to 1.4 ± 0.05 as $U\to\infty$.

The results shown in Fig. 8 are for $\epsilon_f=0$. We have studied short chains to see what happens as ϵ_f drops below zero. In the mixed-valence regime, our study suggests that n_f has the same form as (21) for large U. As ϵ_f becomes more negative, β increases and approaches a value close to 2 for large $|\epsilon_f|$. We show in the Appendix that perturbation theory agrees with this result for $V^2/|\epsilon_f|\ll t$.

D. $U=\infty$

Our renormalization-group approach allows us to study the $U=\infty$ case by eliminating the doubly occupied f states from the Hilbert space. This allows us to compare our results to the predictions of approximation schemes which are applied in this limit, e.g., the slave boson approach[13] and the Gutzwiller approximation.[11]

We study what happens as we reduce V in the cases when $\epsilon_f=0$ and -0.5. In Fig. 9 we compare the spin gap with the one predicted by the slave boson mean-field technique.[13] For the case $\epsilon_f=0$ shown in Fig. 9(a), there is overall qualitative agreement, although the slave boson mean-field theory overestimates the size of the gap. It is important to point out that the slave boson curve has been calculated using a constant density of states, while the numerical results use a tight-binding density of states. Nevertheless, when $\epsilon_f=0$, both give power-law behavior for small V:[15] $\Delta_s\sim V^4$. For the case $\epsilon_f=-0.5$, the situation is quite different, as can be seen in Fig. 9(b). There is qualitative agreement for V greater than 0.5, but then the slave boson curve drops very rapidly for small V. A similar situation can be seen in Figs. 10(a) and 10(b) for $1-n_f$.

To understand these results let us take a closer look at the slave boson mean-field solution.[13] The number of slave bosons $\sum_i b_i^{\dagger}b_i$ represents the number of sites with no f electrons. Each site is subject to the constraint

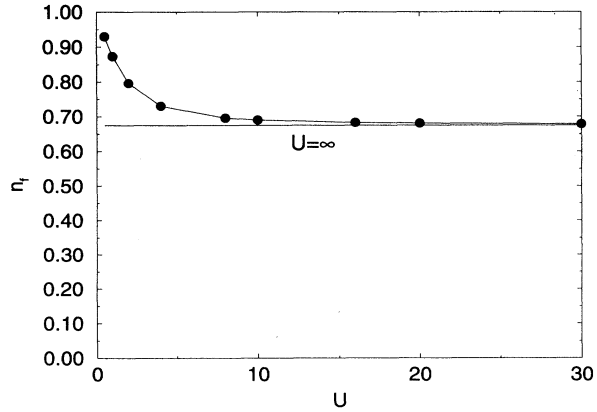

FIG. 8. Occupation n_f of the f level vs U for $L=\infty$ in the asymmetric case ($t=1, V=1, \epsilon_f=0$). As $U\to\infty$, n_f approaches a value close to 0.7.

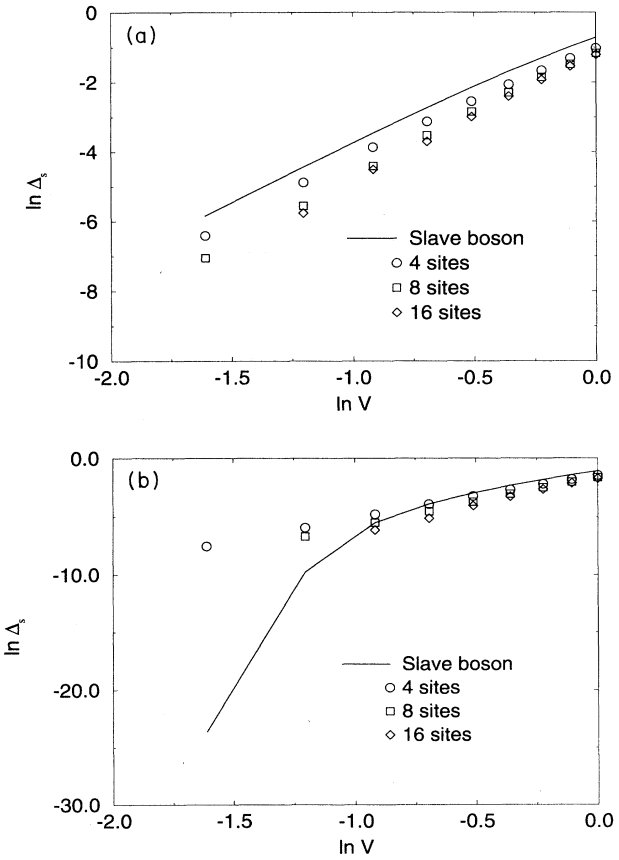

FIG. 9. (a) $\ln(\Delta_s)$ vs $\ln(V)$ for the $U=\infty$ case ($t=1, \epsilon_f=0$). The slave boson results agree qualitatively with our numerical results. (b) $\ln(\Delta_s)$ vs $\ln(V)$ for the $U=\infty$ case ($t=1, \epsilon_f=-0.5$). For small V, the slave boson results deviate significantly from our data.

$$b_i^\dagger b_i + \sum_\sigma f_{i,\sigma}^\dagger f_{i,\sigma} = 1 \ . \tag{22}$$

Since the slave boson number operator is positive definite, each site is constrained to have less than one f electron. In the mean-field approximation the boson operator is approximated by its mean value a_0, i.e., $b_i^\dagger = b_i = a_0$, where a_0 is a real number. This amounts to suppressing double occupancy of the f level only on average. Using slave bosons, an effective Hamiltonian can be written in which doubly occupied sites have been projected out. As a result, there is no U term. The resulting effective Hamiltonian is then equivalent to the $U=0$ Anderson Hamiltonian (3) with an effective hybridization

$$V_{\rm eff}^2 = V^2 a_0^2 = V^2(1-n_f) \ . \tag{23}$$

The slave boson technique recovers the expected picture of two hybridized bands with a gap. The expression for the gap is the same as for the $U=0$ Anderson Hamiltonian with this effective hybridization. For small V, the gap goes as $V_{\rm eff}^2/t$. The f level is also renormalized to $\tilde{\epsilon}_f$ and self-consistent equations for both $\tilde{\epsilon}_f$ and a_0 can be obtained.[13] The small-V expansion of the self-consistent equations gives

$$\tilde{\epsilon}_f = 2ta_0^2 \ ,$$
$$a_0^2 = \frac{4t^2}{V^2} \exp\left[\frac{2t(\epsilon_f - \tilde{\epsilon}_f)}{V^2}\right] \ . \tag{24}$$

When $\epsilon_f < 0$ and V is small enough such that a_0 is very small, then $\tilde{\epsilon}_f$ in the exponential can be neglected and a_0 goes to zero as $\exp(-2t|\epsilon_f|/V^2)$. Thus the gap will depend exponentially on V. When $\tilde{\epsilon}_f$ becomes greater than ϵ_f, $a_0^2 = 1-n_f$ crosses over from exponential to power-law behavior. If $|\epsilon_f| \ll \tilde{\epsilon}_f$, then ϵ_f in the exponent of Eq. (24) can be neglected. Plugging in $\tilde{\epsilon}_f = 2ta_0^2$ gives a transcendental equation for a_0. Solving this numerically, we find that $a_0^2 \sim V^2$. As a consequence, the gap goes as V^4. Thus the slave boson mean-field approach predicts that the gap crosses over from exponential dependence on V to power-law dependence as ϵ_f approaches 0 from below. However, our numerical-renormalization-group results do not show such a change in behavior. Although it might be argued that finite-size systems will give power-law rather than exponential behavior, increasing the length of the chain does not indicate any evidence of such a dramatic crossover. In addition, perturbation theory for an infinite chain shows that $1-n_f$ goes as V^2 when $V^2/\epsilon_f \ll t$ (see the Appendix). This is exactly what we find for $\epsilon_f = -0.5$ with small V.

The reason for this disagreement between the slave boson calculation and the numerical-renormalization-group approach may be that the mean-field approximation neglects spin fluctuations. Spin fluctuations are crucial in the Kondo regime. They also give rise to RKKY interactions.

The $U=\infty$ limit has also been treated by the Gutzwiller approximation.[11] It predicts a ferromagnetic ground state when the system goes towards the Kondo regime where $V^2/\epsilon_f t \ll 1$. However, Rice and Ueda[11] only considered uniform magnetic states, as opposed to antiferromagnetic states, which are favored by RKKY interactions. Using a saddle-point formulation of the Gutzwiller method, Reynolds, Edwards, and Hewson[35] suggest that the Gutzwiller approximation is biased too much in favor of a ferromagnetic state. However, they still find a ferromagnetic instability in the Kondo regime. We do not see any evidence of ferromagnetism in any of the cases we studied. We always find an $S=0$ ground state. We find that strong antiferromagnetic correlations appear as the system goes towards the Kondo regime.

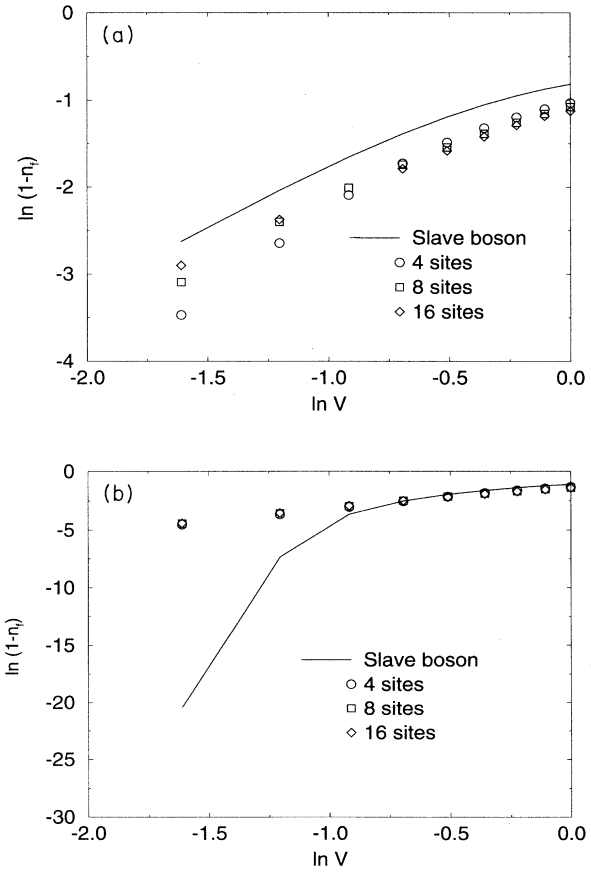

FIG. 10. (a) $\ln(1-n_f)$ vs $\ln(V)$ for the $U=\infty$ case ($t=1, \epsilon_f=0$). The slave boson results agree qualitatively with our numerical results. (b) $\ln(1-n_f)$ vs $\ln(V)$ for the $U=\infty$ case ($t=1, \epsilon_f=-0.5$). For small V, the slave boson results deviate significantly from our data.

V. CONCLUSIONS

We have studied the one-dimensional Anderson lattice at half filling using the density-matrix numerical-renormalization-group technique. We considered the symmetric Anderson model with $\epsilon_f = -U/2$, as well as the asymmetric case in which we set $\epsilon_f = 0$ in order to study the mixed-valence regime. Since many real materials lack particle-hole symmetry and are likely to be in the mixed-valence regime, we concentrated on the asym-

metric model with $\epsilon_f=0$. Our results suggest that some Kondo insulators behave as mixed-valence systems and therefore should be modeled by the Anderson lattice model in the mixed-valence regime as opposed to the Kondo lattice or the Anderson lattice in the Kondo regime.

For all the values of the parameters that we have used, including $\epsilon_f \leq 0$ in the asymmetric case, we find that this is an insulating system with gaps. As $U \rightarrow \infty$ in the symmetric case, the conduction electrons decouple from the f electrons and the gaps approach the values that they have for free electrons. However, in the asymmetric case the gaps approach a finite value in the large-U limit because the conduction electrons do not decouple from the f electrons. There is hybridization due to charge fluctuations into and out of the band of local orbitals whose energy is at or near the Fermi energy.

In both the symmetric and asymmetric cases we find that the charge and quasiparticle gaps are larger than the spin gap for $U>0$. However, we found that the relative values are different in each case. For the mixed-valence case the ratio between the charge gap and the spin gap is roughly 2 in the strong-coupling regime (large U). This is in agreement with Ref. 28, in which the authors report a ratio between the charge gap and the spin gap of $Ce_3Bi_4Pt_3$ equal to 1.8. In contrast, the strong-coupling limit of the symmetric case (Kondo regime) gives a much larger ratio between the two gaps. In fact, it was shown by Nishino and Ueda[6] that this ratio diverges as the Coulomb interaction U goes to infinity. Our result, together with the fact that the occupation of the localized orbital is 0.865 at $T=0$,[10] suggests that $Ce_3Bi_4Pt_3$ behaves like a mixed-valence compound at low temperatures.

In the asymmetric case the nature of the lowest-lying charge excitation changes as U increases. For small U the charge state is made out of two spin-$\frac{1}{2}$ excitations, while for larger U, it becomes a state consisting of two spin-1 excitations. The fact that the gaps are smaller for large U than for $U=0$ is consistent with the fact that band-structure calculations on FeSi,[29,30] which ignore many-body correlations, predict values for the gap that are larger than the optical gap measured experimentally.[31]

We have studied the RKKY interactions by calculating the f-spin–f-spin correlation function as well as the staggered susceptibility $\chi(q)$. We find that the amplitude of the RKKY oscillations decays exponentially with distance. For the symmetric Anderson model, the RKKY interactions become important in the strong-coupling regime ($8V^2/U \ll t$). This can be seen, for example, in the divergence of the susceptibility $\chi(q=2k_F)$ as $U \rightarrow \infty$. This stands in sharp contrast to the asymmetric case in the mixed-valence regime where the RKKY correlations are strongly suppressed due to the reduction in the f occupancy. This agrees with Varma's argument[8] that magnetic correlations are suppressed in the mixed-valence case. Our findings are also consistent with neutron-scattering results on CeNiSn,[9] which found $\chi(q)$ independent of q. Further experiments would be necessary to confirm that CeNiSn is a mixed-valence compound. One such measurement would be photoemission, which can measure the occupation of the f level. In the mixed-valence case that we consider (the localized level right at the Fermi energy and $\Gamma \sim 1$), we find that n_f varies from 1 at $U=0$ to a value close to 0.7 at $U=\infty$.

ACKNOWLEDGMENTS

We would like to thank Steve White, Hervé Carruzzo, Andy Millis, Luiz Oliveira, Doug Scalapino, George Gruner, Kazuo Ueda, and John Wilkins for helpful discussions. This work was supported in part by ONR Grant No. N000014-91-J-1502 and an allocation of computer time from the University of California, Irvine. C.C.Y. would like to thank the Alfred P. Sloan Foundation for financial support.

APPENDIX

In this appendix we use perturbation theory to show that for small V, $1-n_f \sim V^2$ for $U=\infty$. We also show that $n_f(U)-n_f(U=\infty) \sim U^{-2}$. Consider the Anderson Hamiltonian (3) for the case where the hybridization matrix element is zero, i.e., $V=0$, $\epsilon_f<0$, and $\epsilon_f+U>0$. In this case the ground state consists of a half-filled system with one electron per site in the f band. The f-electron states are degenerate with respect to their spin configurations.

For $V>0$ but $V^2/2t|\epsilon_f+U| \ll 1$ and $V^2/2t|\epsilon_f| \ll 1$, perturbation theory can be used to calculate the correction to the ground-state energy. The first nonzero contribution is the second-order term

$$\Delta E_0 = \sum_{m \neq 0} \frac{|\langle m|H_1|0\rangle|^2}{E_0 - E_m} , \tag{A1}$$

where H_1 is the hybridization term. The only possible states that contribute to the sum are those that have one hole in the Fermi sea and an extra electron in the f band or vice versa. Also, the fact that $k_F a = \pi/2 = \pi - k_F a$ allows one to write these two contributions under the same sum:

$$\Delta E_0 = V^2 \sum_{k>k_F} \left[\frac{1}{\epsilon_f - \epsilon_k} - \frac{1}{\epsilon_k + \epsilon_f + U} \right] , \tag{A2}$$

where ϵ_k is the energy of the conduction band. In our case, $\epsilon_k = -2t\cos(ka)$. For the symmetric case $\epsilon_f = -U/2$, this expression coincides with the one obtained by Blankenbecler *et al.*[7] The total ground-state energy to second order is given by

$$e_0 = \frac{E_0}{N} = \epsilon_f + \frac{\sum_{k<k_F} \epsilon_k}{N} + \frac{\Delta E_0}{N} . \tag{A3}$$

The occupation of the f orbital can be obtained by the relation

$$n_f = \frac{\partial e_0}{\partial \epsilon_f} = 1 - \frac{V^2}{N} \sum_{k>k_F} \left[\frac{1}{(\epsilon_k + \epsilon_f + U)^2} + \frac{1}{(\epsilon_f - \epsilon_k)^2} \right] . \tag{A4}$$

For $U=\infty$, this expression gives

$$1-n_f(U=\infty)=\frac{V^2}{N}\sum_{k>k_F}\frac{1}{(\epsilon_f-\epsilon_k)^2}\ . \tag{A5}$$

This implies that for small V, $1-n_f\sim V^2$. Note that for arbitrary U

$$n_f(U)-n_f(U=\infty)=\frac{V^2}{N}\sum_{k>k_F}\frac{1}{(\epsilon_k+\epsilon_f+U)^2}\ . \tag{A6}$$

Thus, for large U, $n_f(U)-n_f(U=\infty)\sim U^{-2}$.

[1]G. Aeppli and Z. Fisk, Comments Condens. Matter Phys. **16**, 155 (1992).
[2]H. Tsunetsugu *et al.*, Phys. Rev. B **46**, 3175 (1992).
[3]Z. Wang, X.-P. Li, and D.-H. Lee, Phys. Rev. B **47**, 11 935 (1993).
[4]C. C. Yu and S. R. White, Phys. Rev. Lett. **71**, 3866 (1993).
[5]R. M. Fye, Phys. Rev. B **41**, 2490 (1990).
[6]T. Nishino and K. Ueda, Phys. Rev. B **47**, 12 451 (1993).
[7]R. Blankenbecler, J. R. Fulco, W. Gill, and D. J. Scalapino, Phys. Rev. Lett. **58**, 411 (1987).
[8]C. M. Varma, Phys. Rev. B **50**, 9952 (1994).
[9]T. E. Mason *et al.*, Phys. Rev. Lett. **69**, 490 (1992).
[10]G. H. Kewi, J. M. Lawrence, and P. C. Canfield, Phys. Rev. B **49**, 14 708 (1994).
[11]T. M. Rice and K. Ueda, Phys. Rev. Lett. **55**, 995 (1985); Phys. Rev. B **34**, 6420 (1986).
[12]C. M. Varma, W. Weber, and L. J. Randall, Phys. Rev. B **33**, 1015 (1986); see also C. M. Varma, in *Moment Formation in Solids,* Vol. 117 of *NATO Advanced Study Institute, Series B: Physics,* edited by W. Buyers (Plenum, New York, 1985), p. 83.
[13]P. S. Riseborough, Phys. Rev. B **45**, 13 984 (1992).
[14]A. J. Millis and P. A. Lee, Phys. Rev. B **35**, 3394 (1987).
[15]R. Jullien and R. M. Martin, Phys. Rev. B **26**, 6173 (1982).
[16]J. Callaway, J. W. Kim, and L. Tan, Phys. Rev. B **48**, 11 545 (1993).
[17]S. R. White, Phys. Rev. B **48**, 10 345 (1993).
[18]S. R. White, Phys. Rev. Lett. **68**, 3487 (1992).
[19]S. R. White and David A. Huse, Phys. Rev. B **48**, 3844 (1993).
[20]E. S. Sørensen and I. Affleck, Phys. Rev. Lett. **71**, 1633 (1993).
[21]R. P. Feynman, *Statistical Mechanics* (Benjamin, Reading, MA, 1972), Chap. 2.
[22]Zs. Gulácsi, R. Strack, and D. Vollhardt, Phys. Rev. B **47**, 8594 (1993).
[23]J. R. Schrieffer and P. A. Wolff, Phys. Rev. **149**, 491 (1966).
[24]M. A. Ruderman and C. Kittel, Phys. Rev. **96**, 99 (1954).
[25]K. Ueda, H. Tsunetsugu, and M. Sigrist, Phys. Rev. Lett. **68**, 1030 (1992).
[26]A. J. Millis (private communication).
[27]M. M. Steiner, R. C. Albers, D. J. Scalapino, and L. J. Sham, Phys. Rev. B **43**, 1637 (1991).
[28]B. Bucher, Z. Schlesinger, P. C. Canfield, and Z. Fisk, Phys. Rev. Lett. **72**, 522 (1994).
[29]C. Fu, M. P. C. M. Krijn, and S. Donaich, Phys. Rev. B **49**, 2219 (1994).
[30]L. F. Mattheiss and D. R. Hamann, Phys. Rev. B **47**, 13 114 (1993).
[31]Z. Schlesinger *et al.*, Phys. Rev. Lett. **71**, 1748 (1993); L. Degiorgi *et al.* (unpublished).
[32]C. M. Varma, Rev. Mod. Phys. **48**, 219 (1976); S. Doniach, Physica B (Amsterdam) **91B**, 231 (1977).
[33]H. R. Krishna-murthy, J. W. Wilkins, and K. G. Wilson, Phys. Rev. B **21**, 1044 (1980).
[34]The value of n_{fi} is much closer to $n_f(L=\infty)$ at sites in the center of the lattice than at sites near the ends. From Eq. (20), we see that the contribution to n_f from sites near the ends fall off as $1/L$.
[35]A. M. Reynolds, D. M. Edwards, and A.C. Hewson, J. Phys. Condens. Matter **4**, 7589 (1992).
[36]C. C. Yu and S. R. White, Physica B **199&200**, 454 (1994).